Type of the Paper (Article)

Investigation of the Mediterranean Cyclone Cleopatra using the WRF model: Sensitivity analysis and ensemble forecasting approach

Markos P. Mylonas, Kostas C. Douvis, Iliana D. Polychroni, Nadia Politi and Panagiotis T. Nastos*

Laboratory of Climatology and Atmospheric Environment, Faculty of Geology and Geoenvironment, National and Kapodistrian University of Athens, University Campus, GR 15874 Athens, Greece.
* Correspondence: nastos@geol.uoa.gr; Tel.: +30 210 7274191

Abstract: Towards the investigation and further understanding of the development and propagation of Medicanes, this study explores the forecasting capability of WRF model in case of cyclone "Cleopatra" which affected with extreme rainfall and strong winds Sardinia and Calabria, Italy, in November 2013. This cyclone was unusual in that it developed a warm core but did not fulfill its transformation into a tropical-like cyclone because its core did not expand high enough in the tropospnere. The ERA5 reanalysis dataset was dynamically downscaled from 31 km spatial horizontal resolution to 9 km using WRF model. The methodology consists of; firstly, an extensive physical parameterization schemes sensitivity test and consequently, a short-range ensemble forecasting implementation based on the highest statistical scored physics configuration. All simulation results were validated against surface observations and remote sensing products. Subsequently, the modeled cyclone trajectories are compared to satellite imagery derived from EUMETSAT-SEVIRI gridded data. The findings of the conducted analysis illustrate that ensemble average displays significant difference in performance compared to any of the deterministic runs individually, suggesting that ensemble forecasts will be beneficial in studies assessing cyclonic events in the Mediterranean region.

Keywords: WRF, Medicane, extra-tropical cyclone, hybrid cyclone, sensitivity analysis

1. Introduction

The Mediterranean basin is an area particularly prone to the generation of low-pressure systems [1]. The dominant type is extra-tropical cyclones, fueled by the baroclinic instability due to horizontal temperature gradients. Extra-tropical cyclones have the potential to develop dangerous weather such as floods and windstorms, particularly when they undergo explosive intensification [2].

However, cyclones with tropical features similar to those of tropical cyclones developed in the Caribbean - South America, Southeast Asia and elsewhere are observed occasionally. Given their similarity to tropical storms, they are referred to as "medicanes" (from the composition of the words MEDIterranean and hurriCANES). They are also often referred to as Tropical-Like Cyclones (TLCs) due to their distinct differences to tropical storms. Medicanes are relatively rare phenomena, occurring about 1.6 times per year [3]. Given their rarity and the fact that they spend most of their lifetime over the sea, their tropical characteristics were not discovered until the 1980's [3]. Medicanes can have serious impacts for the coastal areas and maritime activities of the Mediterranean as documented by [4], including floods caused by heavy rainfall and storm surge, crop disasters, drops of trees from strong winds as well as disasters in natural environment, especially tourist regions.

These phenomena may also cause loss of human lives and destructive consequences in private and public property.

Medicanes are warm-core low-pressure systems, driven by the hydrostatic instability of the atmosphere and the evaporation from the sea surface over which they are formed. They are characterized by axial symmetry and the absence of fronts. Strong winds approach the center circularly and rise around it creating a spiral wall of clouds that surrounds the "eye", a small area with no clouds and no wind, like in tropical storms. The winds typically keep getting stronger until the medicane reaches land, while the stage of the most intensive convection, rainfall and lightning activity happens earlier [5]. They have been found to develop above waters as cold as 15°C, unlike tropical cyclones whose limit is considered to be 26°C [6]. A cold-core cut-off low in the mid-upper levels of the atmosphere has been detected near several medicanes [5,7]. Its presence creates a cold lake aloft, thus enhancing the atmospheric instability and medicane development. This is a major difference to the tropical cyclones whose instability is fueled by the high SSTs [7,8].

One more important difference to the tropical cyclones is that most medicanes, if not all, are initially formed as baroclinic cyclones, which is the dominant type of cyclones in the region. In an advanced stage of their life [8,9] they are converted into acquiring tropical characteristics because of the environmental conditions [10–13]. In this sense they can be classified near the subtropical cyclones [14]. In recent years the process of tropicalization has been the focus of several authors. [13], studying "probably the deepest medicane on record" pointed out the importance of the upper-level jet in the intensification of the system. However, in most medicane cases an upper-level jet is not present [9]. Also, a potential vorticity anomaly in the upper-levels above the surface pressure low was proposed as a trigger for medicane creation. When the two coincide, they cause the surface circulation to intensify, thus enhancing the surface latent heat fluxes into being able to maintain the convection [11,12,15,16].

The geometric and physical characteristics of the Mediterranean basin prevent Medicanes from reaching the size and intensity that tropical cyclones are known to reach. When they leave the sea they lose their energy source, they begin to diminish gradually and soon they disappear. Therefore, most Medicanes travel less than 3,000 km after less than 3 days. As a result, their radius and sustained winds usually do not exceed 200 km and 40 m/sec respectively [5,17]. This wind speed would classify them in Category 1 of the Saffir-Simpson hurricane scale. Although significant progress has been made towards the understanding of medicanes, it is lagging behind in comparison to our understanding of tropical cyclones [18], particularly concerning the process of acquiring tropical characteristics [12,19]. This is not surprising given the much later beginning of their investigation and the much smaller number of historical data that are available for studying.

In recent years it has become clear that some low-pressure systems cannot be classified in the two classic categories, extra-tropical and tropical. There are cases of systems that switch category. Also, there are cases of extratropical cyclones, called "hybrid", inside of which a warm core is developed. Sometimes this happens as a stage of a tropical conversion. The tool typically used for the classification of cyclones in the two main categories, extra-tropical and tropical, or in the gray area around them is the Hart diagrams [20]. They are based on a phase space of parameters that can be deduced if the 3-D structure of the cyclone is known with enough detail to calculate the lower-tropospheric thickness asymmetry (frontal nature) and the tropospheric thermal wind (cold-core versus warm-core structure) in a low (900-600 hPa) and a high (600-300 hPa) layer. The position and trajectory of a cyclone in the phase space can determine if it is a clear case of tropical or extra-tropical cyclone or if it undergoes a change or if it has a hybrid structure. The method can be applied in the Mediterranean, although the calculations must be performed on a smaller area than a circle with a 500 km radius around the low-pressure center, i.e. in a radius of 200 km [13,21] or 150 km [10] or so.

Several authors have used limited area models to simulate historical medicanes aiming at a better understanding of the phenomenon or at investigating the capability of numerical weather prediction to capture its occurrence and development. This method is considered to have a potential to generate valuable results. Being a mesoscale phenomenon, medicanes require high-resolution simulations in order to be accurately represented [9,13,17,22–25]. Increasing resolution improves the

 doi:10.20944/preprints201810.0196.v1

results, i.e. [26] performing nested LAM simulations found that at about 50 km resolution a medicane is not detected, at 25 km a pressure low with a warm core is detected but it is poorly represented, and at 9 km most medicane features can be reproduced and be well resolved. Also, there is a need for high-resolution SST fields spatially and temporally, either the ocean is coupled or prescribed [27].

The good quality of initial and boundary conditions is a key for accurate simulation of the occurrence and development of medicanes [27,28]. Besides, the use of a domain large enough and an initiation time early enough to capture the entire formation of the vortex has been proposed [28]. They found that even when the simulation runs on global forecast output, this configuration allows for better results than the usage of more recent output. This poses an obstacle on the real-time forecast of occurrence and development of medicanes because more computational resources and more time are required.

The development and the trajectory of medicanes depend mostly on the forcing, the internal structure and intensity depend mostly on the model configuration [28]. Coupled ocean-atmosphere models produce better than atmosphere-only models with prescribed SST when the atmospheric resolution is high [26]. Further, the strong impact on the results has been stressed by the choice of PBL scheme and of the dependence of the waves on surface roughness, especially when the medicanes approach the coast, which should be treated by sensitivity tests [27].

In the present study the Weather Research and Forecasting model is used to study the Mediterranean cyclone "Cleopatra". It was a cyclone that produced extreme weather that devastated parts of Italy causing severe damages and claiming 18 lives in November of 2013. This is not the only reason that makes "Cleopatra" worth studying. It was an extra-tropical cyclone that, in a mature stage of its life developed a warm core. However, the warm core did not grow to become dominant thus transforming the cyclone into a medicane. It remained a hybrid cyclone. This cyclone that dwells in the grey area between the typical extra-tropical type and the tropical-like cyclones is an ideal testbed for the study of the tropical transition of Mediterranean extra-tropical cyclones. More work on "Cleopatra" is planned in the framework of the project MEDICANE. In view of these plans the present study is a sensitivity test in the use of WRF for the simulation of cyclone Cleopatra and Mediterranean cyclones in general.

Section 2 presents the model and the different configurations that were tested, as well as the observational datasets that were used for the evaluation of the simulations. In section 3 a description of cyclone "Cleopatra", the synoptic situation and its impacts is provided. Also, the results of the sensitivity test simulations and of an ensemble of forecast runs are presented along with a comparison to observations, individually and as an ensemble. In sections 4 and 5 the results are discussed and the conclusions of the study are reiterated.

2. Materials and Methods

The Weather Research and Forecasting mesoscale model (WRF) [29], version 3.9, is used for the simulations of this study. The domain has a 9-km spatial horizontal resolution, focusing on the Mediterranean region, with 336 × 231 grid points (Figure 1). The 50 vertical levels are arranged according to terrain-following hydrostatic pressure vertical coordinates. The time-step is adaptive and based on the horizontal resolutions and it is determined between 54 and 140 seconds.

Preprints (www.preprints.org) | NOT PEER-REVIEWED | Posted: 10 October 2018 doi:10.20944/preprints201810.0196.v1

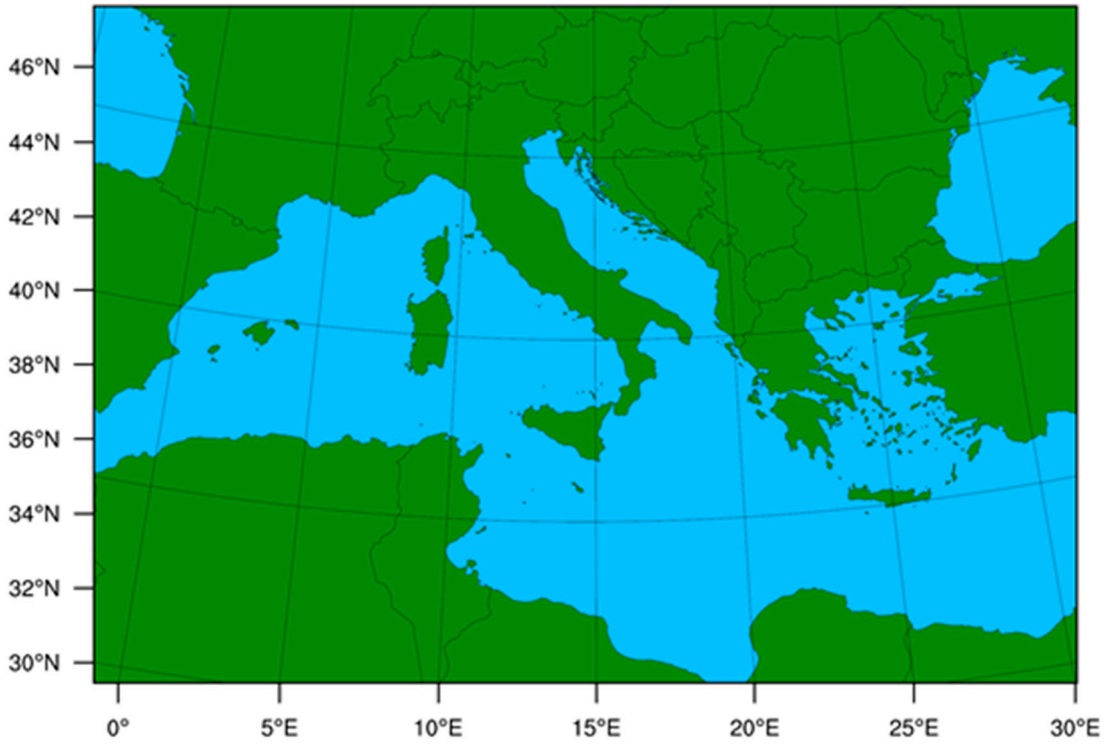

Figure 1. Domain of case study.

A series of sensitivity tests is performed in order to assess the dependence of model performance on the choice of physics parameterization schemes. Fifteen different model setups are tested on their ability to simulate the characteristics of cyclone "Cleopatra". In order to organize the procedure a main configuration is selected (hereafter named "MAIN") and all other configurations differ form MAIN in only one parameterization scheme (and their dependencies in some cases). In total 14 alternative configurations are tested, differing from MAIN in 6 kinds of physical parameterizations as shown in Table 1.

Table 1. WRF simulations' configurations associated with physics parameterization schemes.

Control Setup	setup Main			
Sfclay	setup_1			
PBL	setup_2	setup_3	setup_4	
Microphysics	setup_5	setup_6		
Radiation	setup_7	setup_8	setup_9	setup_10
Cumulus	setup_11			
LSM	setup_12	setup_13	setup_14	

Concerning the Planetary Boundary Layer (PBL) schemes, Yonsei University (YSU) [30], Mellor–Yamada–Janjic (MYJ) [31], Asymmetric Convective Model version 2 (ACM2) [32] and the Mellor-Yamada Nakanishi and Niino Level 2.5 (MYNN2.5) [33] are involved, associated with the corresponding surface layers schemes, which provide the surface fluxes of momentum, moisture and heat to PBL scheme. The Sfclay (surface layer) parameterizations used are the Mellor-Yamada Nakanishi and Niino surface layer scheme (MYNN) [33] and the revised version of MM5 [34]. For compatibility reasons with the MYJ PBL scheme, ETA surface layer is also used [35]. Regarding the cloud microphysics schemes, the four following options are mainly used, WRF single-moment six-class (WSM-6) containing ice, snow and graupel processes [36], Ferrier (FE) and Thompson (THOM), which includes six classes of moisture for ice as prognostic variables [37]. For the land surface model, different setups involve the 5-layer thermal diffusion (5-L Thermal DIF), Noah Land Surface Model [38–40], RUC Land Surface Model and Noah-MP (multi-physics) [41]. The cumulus convection

Preprints (www.preprints.org) | NOT PEER-REVIEWED | Posted: 10 October 2018 doi:10.20944/preprints201810.0196.v1

scheme controls the sub-grid-scale effects of convective clouds and the options is set mainly to Kain–Fritsch (KF) scheme and Grell 3D (G3D) [42,43]. Finally, for the long-wave and short-wave radiation schemes, five different options are used in this case study: 1) New Goddard (New Goddard) [44], 2) RRTM scheme [45] and its newer version of RRTMG schemes [46], 3) Dudhia [47] , only for short-wave scheme, 4) GFDL [48] and 5) Community Atmosphere Model (CAM) scheme [49]. The parameterization schemes used in each one of the sensitivity test simulations is presented in Table 2.

Table 2. Parameterization schemes for physical processes for each of the 15 WRF simulations.

SimID	MIC	LW_RAD	SW_RAD	LSM	Sfsclay	PBL	CUM
MAIN	THOM	New Goddard	New Goddard	5-L Thermal DIF	MYNN	MYNN2.5	KF
SETUP_1	THOM	New Goddard	New Goddard	5-L Thermal DIF	Revised MM5	MYNN2.5	KF
SETUP_2	THOM	New Goddard	New Goddard	5-L Thermal DIF	ETA	MYJ	KF
SETUP_3	THOM	New Goddard	New Goddard	5-L Thermal DIF	Revised MM5	YSU	KF
SETUP_4	THOM	New Goddard	New Goddard	5-L Thermal DIF	Revised MM5	ACM2	KF
SETUP_5	FERRIER	New Goddard	New Goddard	5-L Thermal DIF	MYNN	MYNN2.5	KF
SETUP_6	WSM6	New Goddard	New Goddard	5-L Thermal DIF	MYNN	MYNN2.5	KF
SETUP_7	THOM	RRTM	Dudhia	5-L Thermal DIF	MYNN	MYNN2.5	KF
SETUP_8	THOM	CAM	CAM	5-L Thermal DIF	MYNN	MYNN2.5	KF
SETUP_9	THOM	RRTMG	RRTMG	5-L Thermal DIF	MYNN	MYNN2.5	KF
SETUP_10	THOM	GFDL	GFDL	5-L Thermal DIF	MYNN	MYNN2.5	KF
SETUP_11	THOM	New Goddard	New Goddard	5-L Thermal DIF	MYNN	MYNN2.5	G3D
SETUP_12	THOM	New Goddard	New Goddard	NOAH	MYNN	MYNN2.5	KF
SETUP_13	THOM	New Goddard	New Goddard	RUC	MYNN	MYNN2.5	KF
SETUP_14	THOM	New Goddard	New Goddard	NOAH-MP	MYNN	MYNN2.5	KF

The 15 sensitivity test simulations are initialized on November 17, 2013, 1200 UTC with 12 hours of model spin up time and ended on November 23, 2013, 0000 UTC. The initial and boundary conditions are provided by ERA5 data, derived from the European Center for medium range Forecast (ECMWF). ERA5 dataset has a spatial horizontal resolution of 0.28 x 0.28° (approximately 31 km spacing grid) and temporal resolution of 1 h with 37 isobaric atmospheric levels and 4 below land surface [50].

In addition, the model is tested in forecast mode, using ICBCs from Global Forecasting System (GFS) forecast data, derived from National Oceanic and Atmospheric Administration (NOAA) archive for historical forecasts. GFS dataset has a spatial horizontal of 0.25° x 0.25° and a temporal resolution of 3 h with 42 isobar atmospheric levels and 4 levels below ground [51]. The exact same configuration is used, except that only the four setups that perform best in the sensitivity tests are

Preprints (www.preprints.org) | NOT PEER-REVIEWED | Posted: 10 October 2018 doi:10.20944/preprints201810.0196.v1

used. The WRF/GFS simulations started on November 18, 2013, 0000 UTC and ended on November 23, 2013, 0000 UTC.

Moreover, remote sensing data are used in order to validate the sensitivity simulations. More specifically, Multi-Sensor Precipitation Estimate (MPE), which is most suitable for convective precipitation, as well as Rapid Scan High Rate SEVIRI Level 1.5 Image Data derived from the Spinning Enhanced Visible and InfraRed Imager (SEVIRI) of European Organization for the Exploitation of Meteorological Satellites (EUMETSAT) [52]. The latter is used to derive the cyclone center positions as well as the cloud-top brightness temperature (BT) from the infrared 10.8 μm band through the MSGView software [53].

Finally, in order to validate the ensemble forecast simulations, meteorological data concerning Meteorological Terminal Aviation Routine Weather Reports (METARs) are processed, regarding values of surface pressure, air temperature at 2m and surface wind speed at 10m, acquired from the archives of the following four meteorological stations: Olbia (WMO ID:16531) , Brindisi (WMO ID: 16320) and Rome (WMO ID: 16242) installed by the Servizio Meteorologico Aeuronautica Militare of Italy and Zadar (WMO ID: 14428) installed by the Croatian Meteorological and Hydrological Service (DHMZ).

3. Results

The first part of this section includes the description of cyclone Cleopatra, the synoptic situation and the most severe impacts that it caused. In the next parts, the results of the sensitivity experiments to different physics parameterizations are compared to observational datasets. Lastly the results of the ensemble of forecast simulations are evaluated.

3.1. Description of case study

Hybrid cyclone Cleopatra (also named Ruven by the Free University of Berlin) developed in the western Mediterranean basin in 17-19 November 2013 (Figure 2). The cyclone produced some extreme weather in Sardinia and at the tip of the Italian peninsula on the 18th and 19th, respectively. Although Cleopatra did not transform into a medicane, it did develop some tropical activity.

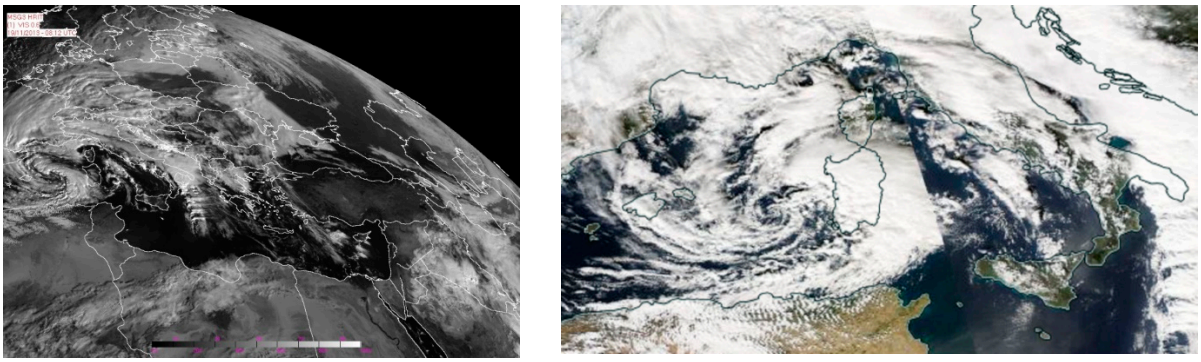

(a) (b)

Figure 2. Satellite images of Cyclone Cleopatra on visible channel from (a) SEVIRI rapid scan and (b) Aqua/Modis on 19 of November 2013.

An elongated 500 hPa trough started developing and was cut off over western Europe since the 14th. The cut-off low retrograded and by the 16th it was located over the Iberian Peninsula where it remained for some days until it started moving east and was absorbed by another trough approaching by the west. The presence of cold air and high potential vorticity associated with the cut-off low stirred the weather in the western Mediterranean for the following days and lead to the development of Cleopatra. The surface low center developed on the 17th in the east of Spain where it remained until it started propagating east, following the upper air cut-off low, towards Sardinia and Italy. This synoptic situation prompted frontal and other mesoscale activity all over the western Mediterranean basin.

Preprints (www.preprints.org) | NOT PEER-REVIEWED | Posted: 10 October 2018 doi:10.20944/preprints201810.0196.v1

The most notable weather events occurred in Sardinia and in Calabria, Italy. In Sardinia a large part of the island received more than 50 mm of rain in one day, on the 18th [54]. A smaller area received more than 400 mm, or about half of the annual precipitation height, most of which in just a few hours in the morning of that day. This resulted in devastating floods in several parts of the island. The water reached up to 3 meters deep affecting thousands of people and killing 18. Damages involved roads, bridges, buildings, agriculture, cars and other public and personal properties. The media mentioned that the cost of the damages reached 1 billion euro. On the 19th the most severe weather hit the region of Calabria, at the southern tip of the Italian peninsula. Precipitation height up to 214.8 mm was observed causing floods and landslides [55]. Damages included submerged cars and houses, as well as problems with roads, railways, energy, water and communications. The area with severe damages was 1380 km², which amounts to 9% of the area of the region.

The tropical transition of Mediterranean cyclone Cleopatra is evidenced by the following: It developed in the area that has generated most TLCs in record [56]. The synoptic environment was favorable in that a cold cut-off low was situated in the upper levels of the atmosphere near it [7,8]. Also, a potential vorticity anomaly in the upper levels was nearby [11,12,15,16]. The tropical transition is illustrated more clearly in Figure 3, which presents the Hart diagram for the thermal wind in the lower tropospheric layer (900-600 hPa, horizontal axis) against the upper tropospheric layer (600-300 hPa, vertical axis). Beginning as an extra-tropical cyclone (lower-left quadrant) a shallow warm core was formed in the lower tropospheric layer (lower-right quadrant) which grew, briefly reaching the upper tropospheric layer (upper-right quadrant), thus completing its tropical transition for several hours. [14] It is worth mentioning that the phase space diagrams for the rest of the configuration setups (not shown) present only minor nuances, suggesting similar behavior regarding the nature of cyclone phase evolution.

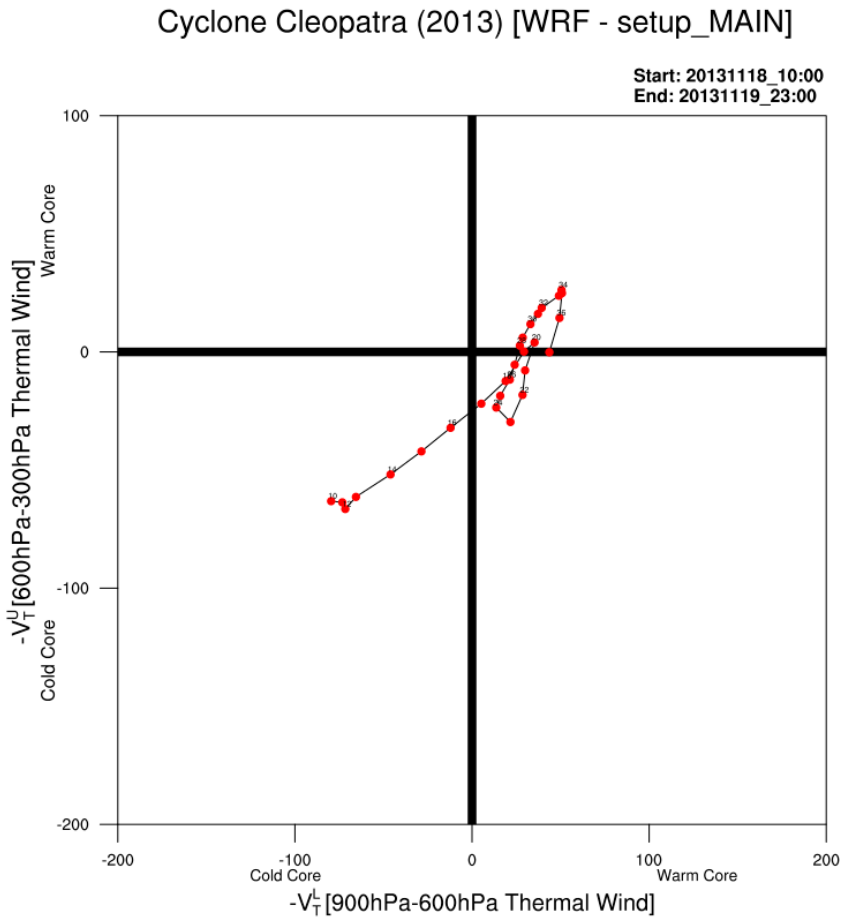

Figure 3. Hart Diagram for setup_MAIN depicting the hourly cyclone space phase evolution $-V_T^L$ vs $-V_T^U$. The starting time is 10 hours after the initialization of the model.

Preprints (www.preprints.org) | NOT PEER-REVIEWED | Posted: 10 October 2018 doi:10.20944/preprints201810.0196.v1

3.2. Sensitivity analysis

In order to assess the dependence of model performance on the physical parameterizations' choice, a sensitivity analysis is performed among the 15 setups described in section 2. The results of the respective 15 simulations performed with ERA5 forcing are described in section 2 and are evaluated against observations.

3.2.1. Trajectories

Figure 4 presents the trajectory, i.e. the low-pressure center locations of the cyclone, as reproduced by the 15 WRF simulations along with the SEVIRI rapid scan imagery locations. The variability among the simulation results is quite limited. Overall, all simulation results reproduce rather well the observed trajectories, spatially and temporally. The beginning and the end of the trajectories in the simulations falls near the observed and their distance remains smaller than 1° throughout the track of the cyclone. The greatest deviation begins over the island of Sardinia where all the model runs simulated a northward shift over the Gennargentu mountain range in southeast Sardinia and ends before the cyclone center reaches the Italian peninsula.

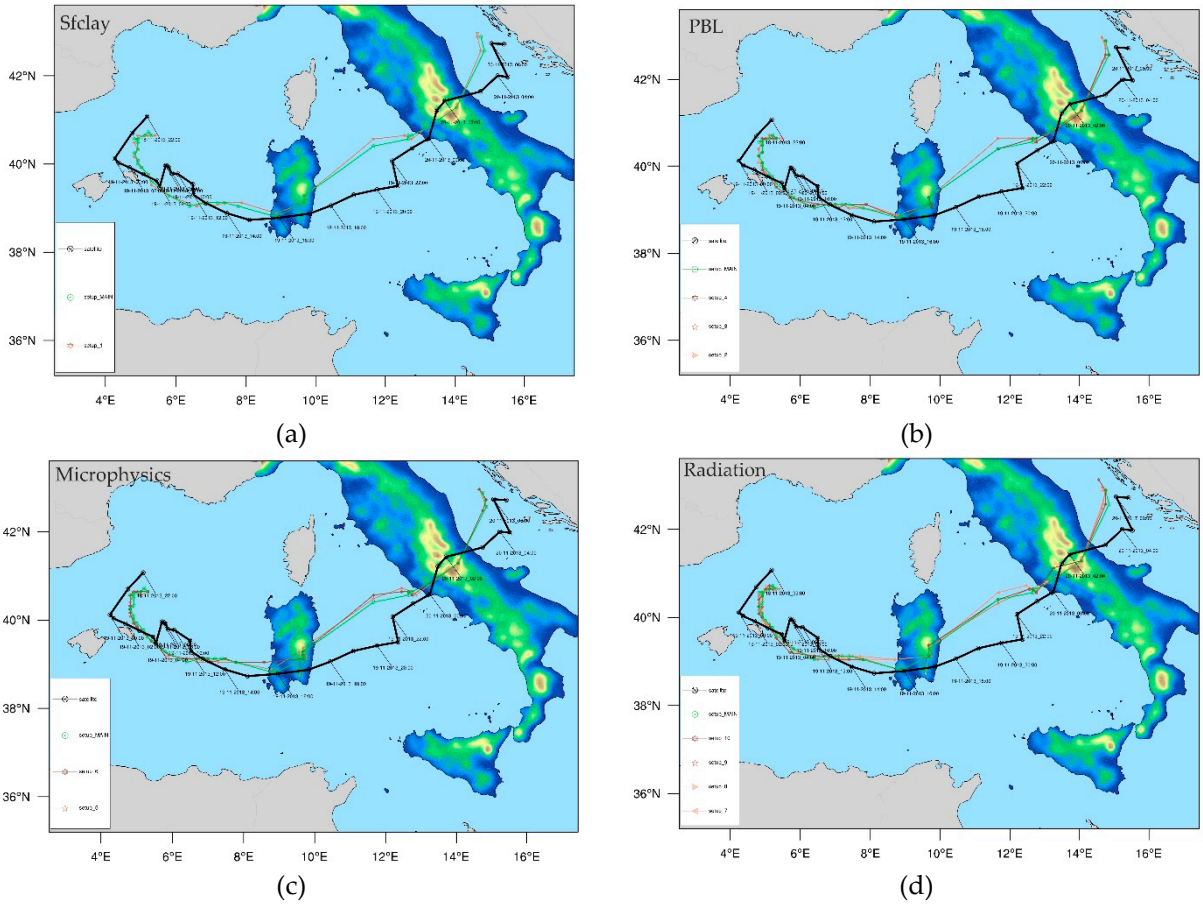

Preprints (www.preprints.org) | NOT PEER-REVIEWED | Posted: 10 October 2018 doi:10.20944/preprints201810.0196.v1

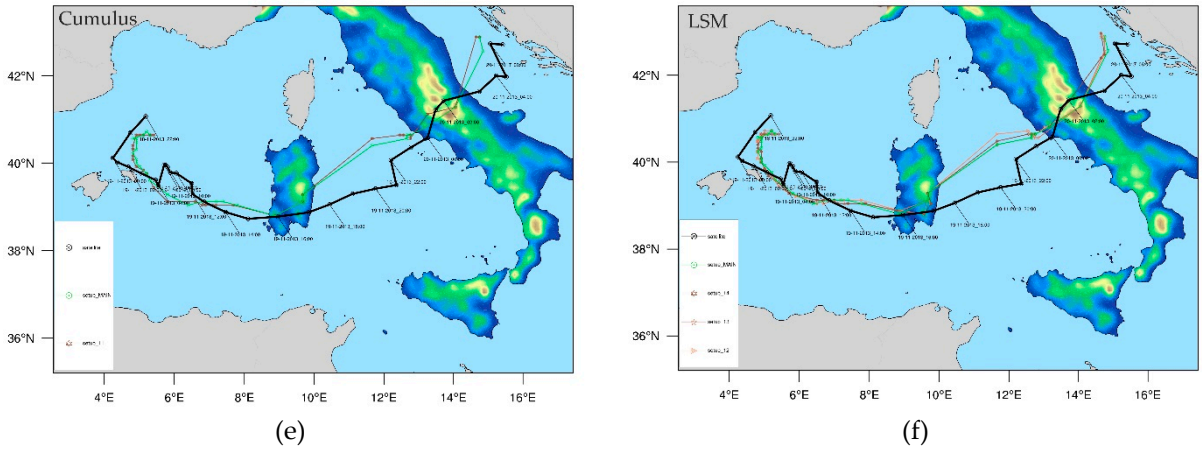

(e) (f)

Figure 4. Trajectory of cyclone Cleopatra in the sensitivity test simulations and in the observations. The grouping of the 15 simulations was based on the type of parameterization that differed from the MAIN configuration in each one: (a) sfclay, (b) PBL, (c) microphysics, (d) radiation, (e) cumulus and (f) LSM schemes. The trajectory of setup MAIN and the trajectory given by SEVIRI rapid scan imagery are represented in all panels with green and thick black lines respectively.

3.2.2. Cloud top temperature (CTT)

Figure 5 presents the Taylor diagrams for the comparison of cloud top temperature (CTT) results with the observations BT. All data points are located in a rather small area, specifically the values of root mean square error (RMSE) vary in the range 4 °C – 5.5 °C and the values of correlation coefficient vary in the range 60% – 80%. According to RMSE the best performing setups are 12, 13, 14 (land surface), 11 (cumulus convection) and MAIN, while the setups performing worse are 2, 3, 4 (planetary boundary layer) and 5 (cloud microphysics). According to the correlation coefficient the setups that perform best are 12, 13, 14 (land surface), 11 (cumulus convection), 6 (cloud microphysics) and 10 (radiation) and the setups that perform worst are 1 (surface layer), 2 (planetary boundary layer), 7 ,8 (radiation) and MAIN. According to standard deviation the setups that fall closest to the observations are 1 (surface layer), 13, 14 (land surface) and MAIN, and the setups that performed worst are 3, 4 (planetary boundary layer), 5 (cloud microphysics), 10 (radiation). Table 3 presents the bias for each of the simulations, also based on the cloud top temperature. The best performing setups were 1 (surface layer), 14, 13 (land surface), 11 (cumulus convection), 7 (radiation) and MAIN. The worst performing setups were 10 (radiation), 2, 3, 4 (planetary boundary layer), 5 and 6 (cloud microphysics),

Overall, the setups that performed best are 13, 14 and 11, followed by 1, 9, 12 and MAIN while the worst performing setups are 2 ,3 ,4 (surface layer), 6 (cloud microphysics) and 8 (radiation). Based on these results setups 9, 11, 13 and MAIN were selected to participate in the forecasting ensemble of the next part of the study. Setup 1 was rejected because its performance on correlation was particularly bad in comparison to the other simulations of the sensitivity study. All setups with different land surface model performed very well, especially 13 and 14. Of those only one, specifically setup 13, was selected to be a member of the ensemble in order to achieve more diversity among the ensemble members.

Table 3. Bias error in °C of the fifteen sensitivity test simulations for cloud top temperature (CTT)

Control Setup	**setup_MAIN** **1.47**		
Sfclay	setup_1 0.62		
PBL	setup_2 3.49	setup_3 3.87	setup_4 4.13
Microphysics	setup_5	setup_6	

Preprints (www.preprints.org) | NOT PEER-REVIEWED | Posted: 10 October 2018 doi:10.20944/preprints201810.0196.v1

	2.03	2.40		
Radiation	setup_7 1.35	setup_8 1.56	**setup_9** **1.61**	setup_10 3.61
Cumulus	**setup_11** **1.13**			
LSM	setup_12 1.9	**setup_13** **1.11**	setup_14 1.01	

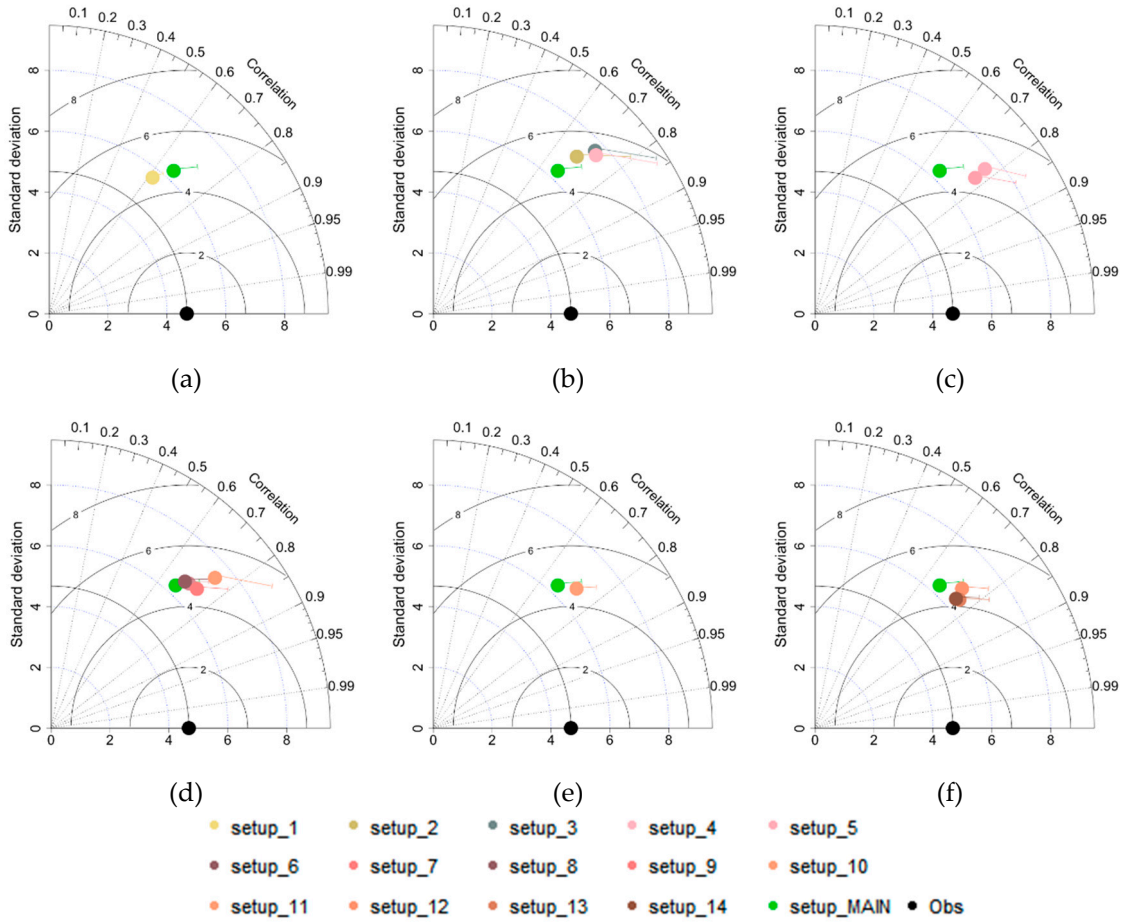

Figure 5. Taylor plots of the cloud top temperature of the sensitivity test simulations. The grouping of the 15 simulations was done based on the type of parameterization that differed from the MAIN configuration in each one: (a) sfclay, (b) PBL, (c) microphysics, (d) radiation, (e) cumulus and (f) LSM schemes. Simulation MAIN is presented in all panels with the green dot. The bar extended from the marker displays a qualificated measurement of the mean error between the respective model and the observed value.

3.2.3. Precipitation

Figure 6 depicts precipitation rate for all 15 sensitivity simulations and for the Multi-Sensor Precipitation Estimate (MPE) observational dataset at 15:00 UTC, November 18th 2013, i.e. in the time of extreme rainfall over Sardinia. Overall, all simulations reproduce reasonably well the position of the fronts and the spatial distribution of precipitation patterns. The differences among the simulation results are insignificant.

Preprints (www.preprints.org) | NOT PEER-REVIEWED | Posted: 10 October 2018 doi:10.20944/preprints201810.0196.v1

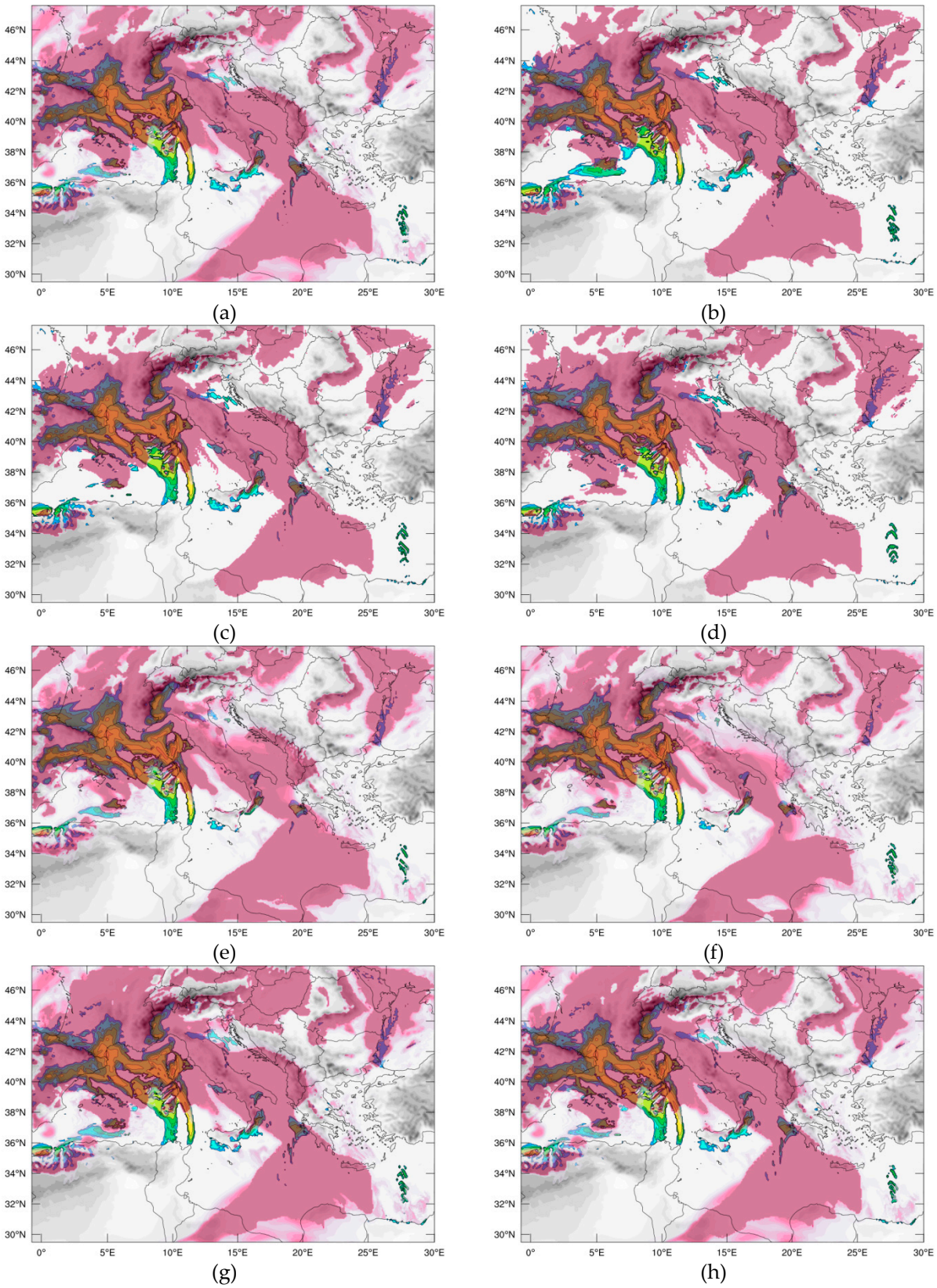

Preprints (www.preprints.org) | NOT PEER-REVIEWED | Posted: 10 October 2018 doi:10.20944/preprints201810.0196.v1

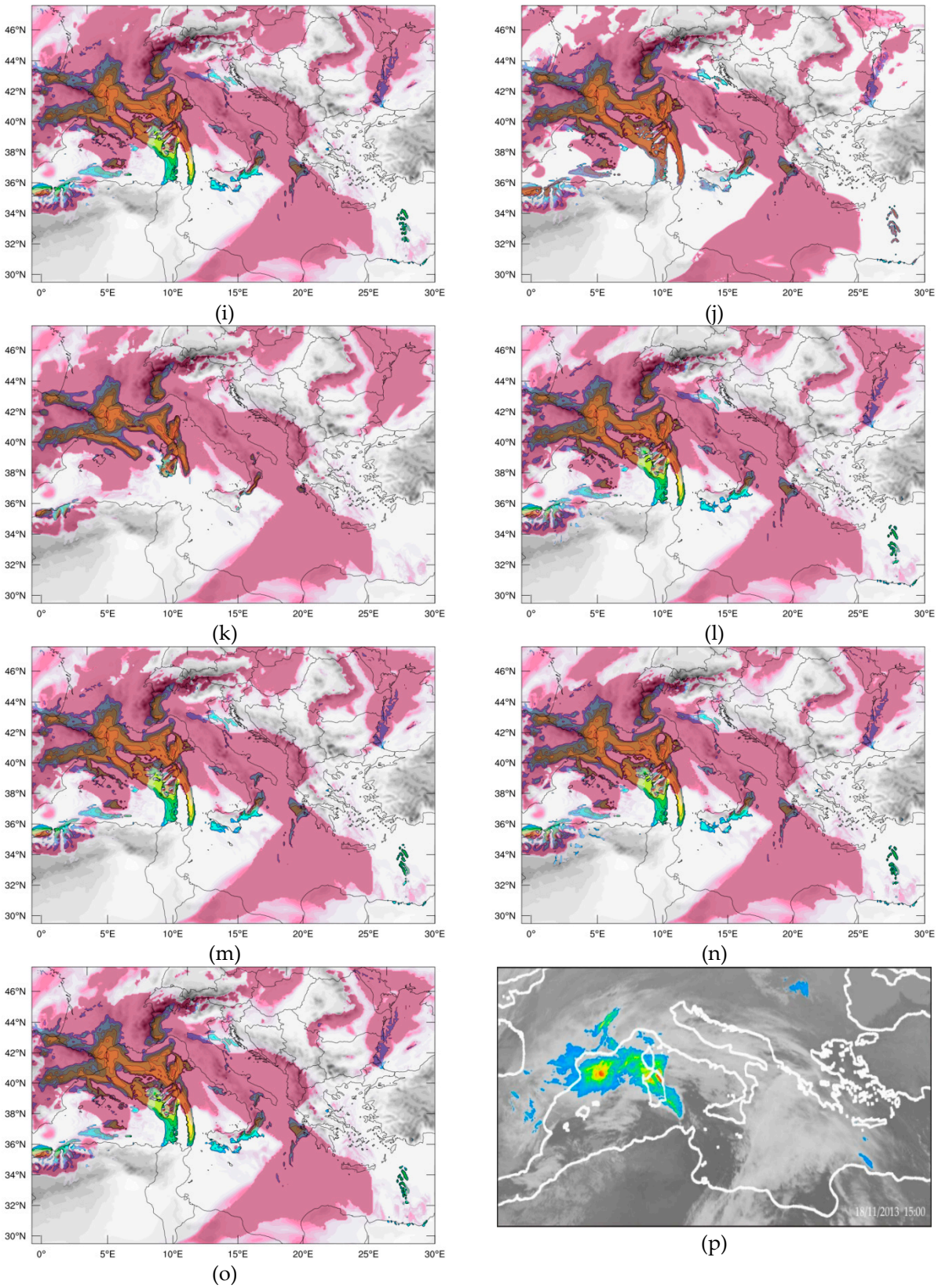

Figure 6. Spatial distribution of precipitation rate at 15:00 UTC on November 18, 2013 according to the 15 simulations and to the Multi-Sensor Precipitation Estimate (MPE) observational dataset derived from EUMETSAT as follows: (a) setup_1, (b) setup_2, (c) setup_3, (d) setup_4, (e) setup_5, (f)

Preprints (www.preprints.org) | NOT PEER-REVIEWED | Posted: 10 October 2018 doi:10.20944/preprints201810.0196.v1

setup_6, (g) setup_7, (h) setup_8, (i) setup_9, (j) setup_10, (k) setup_ 11, (l) setup_12, (m) setup_13, (n) setup_14, (o) setup_MAIN and (p) OBS.

3.3. Forecast ensemble simulation of cyclone "Cleopatra"

In this sub-section the evaluation of the forecast ensemble simulations, forced by GFS data is described.

3.3.1. Trajectories

Figure 7 depicts the trajectory of cyclone "Cleopatra" as simulated by the 4 ensemble members along with the ensemble mean and with the observed trajectory. The ensemble mean is derived by averaging the latitude and the longitude of the location of the sea surface level pressure minima of the four members of the ensemble at all times. The forecast simulations reproduce the cyclone track quite well with a southwest deviation of ~1.5° at the beginning of the forecast which is eliminated when the cyclone reaches Sardinia. Akin to the sensitivity analysis simulations, a northward shift is produced immediately after entering the Tyrrhenian sea, which causes the simulated trajectory to diverge ~1° until it reaches the Italian peninsula. At the same time a 4-hour delay occurs which remains until the end of the cyclone track.

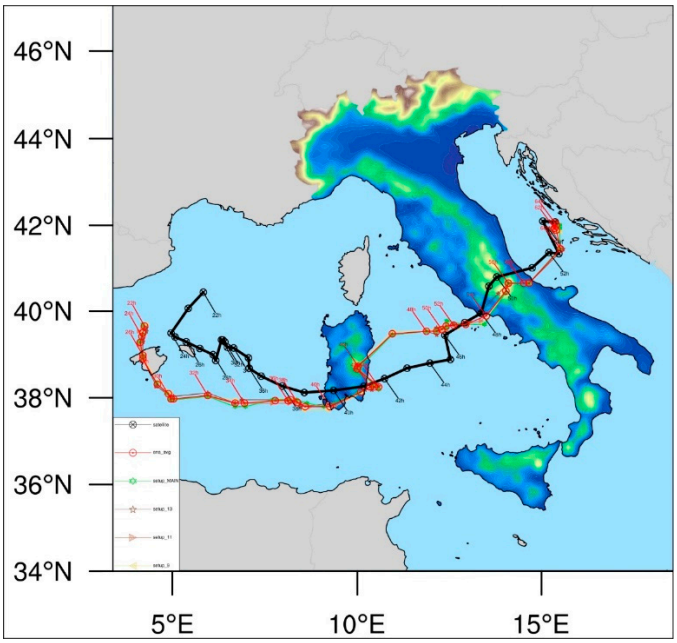

Figure 7. Trajectory of cyclone Cleopatra for all the ensemble members along with the ensemble mean (red line) compared with the observed track (black line).

3.3.2. Surface stations

WRF/GFS simulation results are compared with observations from four METARs stations (Olbia, Brindisi, Rome and Zadar), whose location is inside the affected by cyclone "Cleopatra" areas to verify the coherence of the model fields. Three variables were analyzed: i) mean sea level pressure (MSLP), ii) temperature at 2m and iii) wind speed at 10m. The model time-series are derived by the four nearest grid points to the coordinates of the stations by applying bi-linear interpolation. The comparison of the simulated time-series to the observed ones is presented in the following Figures in the form of Taylor diagrams, with respect to the period from November 18, 2013, 1000 UTC to November 20, 2013, 0700 UTC.

Figure 8 presents the evaluation of mean sea level pressure. The 4 members of the ensemble exhibit a very similar behavior, as all experimental dots are located close to each other. The only exception is the point of setup_9 in Olbia which is located slightly further than the other 3. Overall, the simulations are in good agreement with the observations, with the agreement being strongest in

Preprints (www.preprints.org) | NOT PEER-REVIEWED | Posted: 10 October 2018 doi:10.20944/preprints201810.0196.v1

Brindisi and weakest in Zadar. RMSE values are quite low, less than 3 hPa in all cases. The largest errors are found in Zadar and the smallest in Brindisi, almost 1 hPa. Also, correlation is in all cases higher than 90% (Zadar) and it is as high as 98% in Brindisi. The standard deviation is consistently slightly smaller than the observations in all stations, except in Olbia where it is roughly 25% smaller.

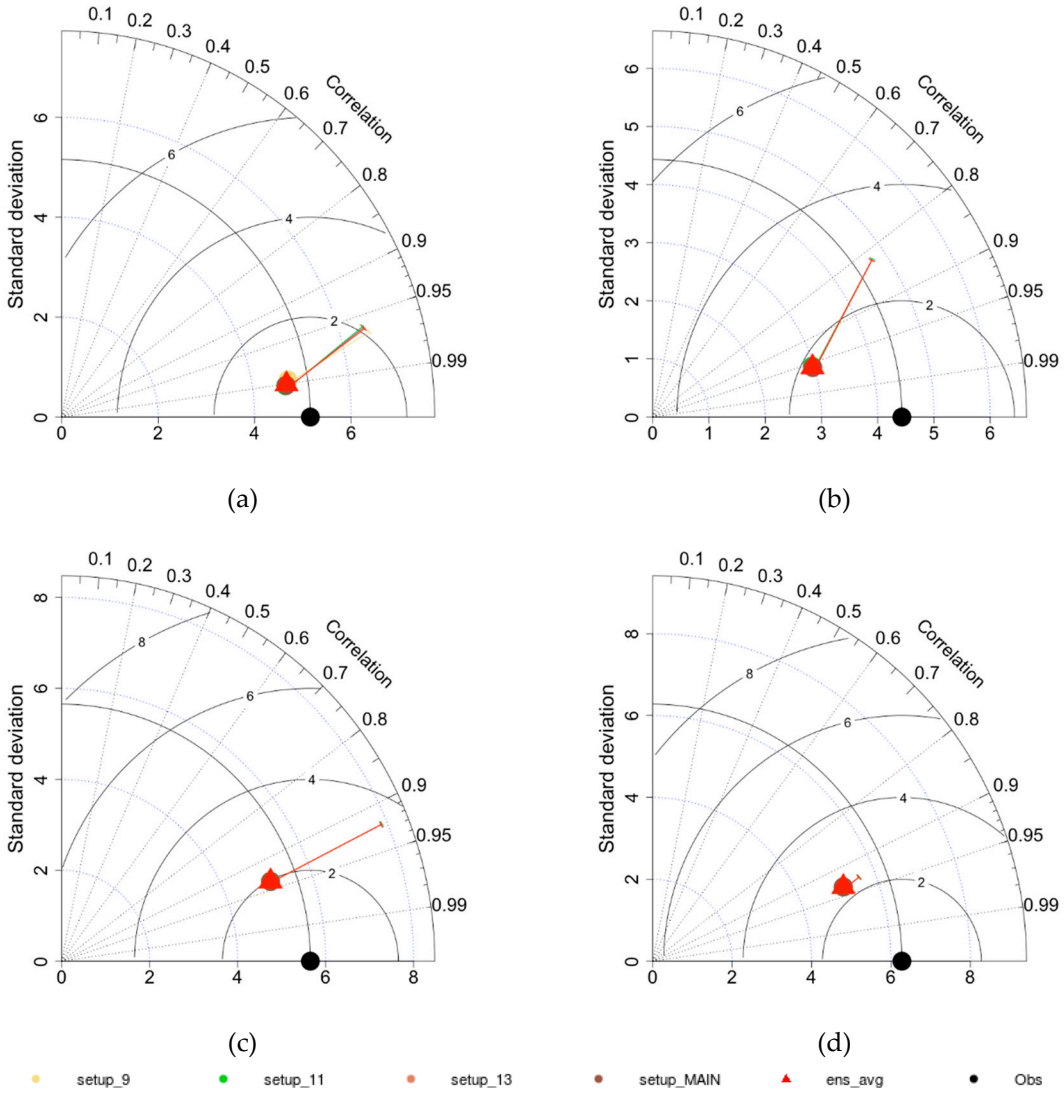

Figure 8. Taylor plots for the comparison of the results of GFS/WRF simulations of setups 9, 11, 13, and MAIN, as well as ensemble mean, against METARs stations' data of (a) Brindisi, (b) Olbia, (c) Rome and (d) Zadar, for mean sea level pressure during the development of cyclone "Cleopatra". The bar extended from the marker displays a qualificated measurement of the mean error between the respective model and the observed value.

In Figure 9 the evaluation of the temperature at 2m time-series is presented. The agreement among the members of the ensemble is not as high as in the previous figure, as the dots are further from each other than in the previous figure. Also, the results are relatively in agreement with the observations, but not as much as in the previous figure. The behavior of the simulations at the location of the 4 stations is similar concerning RMSE and correlation. RMSE values vary roughly in the range 1.5 °C to 2.5 °C with the smallest errors at Rome and the largest errors at Olbia. All correlation values are close to 70%, except for the setup_9 which correlates with the temperature observations of Rome better than 80%. The only metric that exerts significant discrepancy among the 4 stations is the standard deviation, which varies from roughly 40% of the standard deviation of the observations in Brindisi to 120% of the standard deviation of the observations in Zadar. No member of the ensemble

Preprints (www.preprints.org) | NOT PEER-REVIEWED | Posted: 10 October 2018 doi:10.20944/preprints201810.0196.v1

seems to behave better or worse than the others, although the dots are distinguishable, but in Rome the simulations seem to behave slightly better as the RMSE and correlation are slightly better and standard deviation is close enough to the observations'.

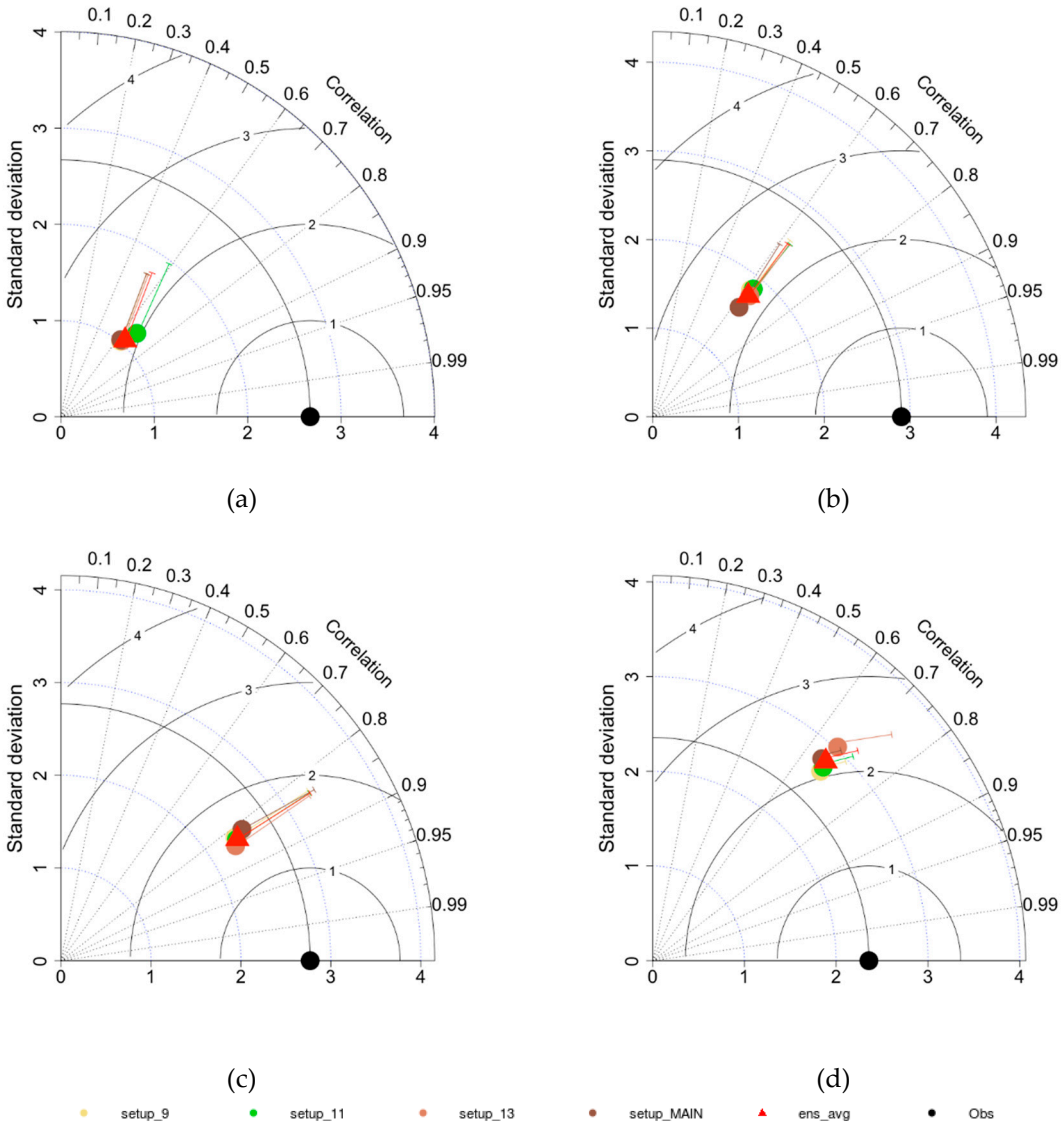

Figure 9. As in Figure 8 except for temperature at 2m.

The evaluation of the time-series of wind at 10m is presented in Figure 10. The differences among the 4 members of the ensemble are moderate relatively to the two previous figures. The RMSE in the four stations varies from roughly 1.25 m/s in Rome to 2.5 m/s in Brindisi and Olbia. Correlations vary more than in the previous figures with values from roughly 35% in Zadar for most models and even 25% for setup_9 to roughly 75% in Brindisi. Standard deviation also exhibits strong variability among stations from about 35% of the standard deviation of the observations in Zadar to 170% in Olbia.

Preprints (www.preprints.org) | NOT PEER-REVIEWED | Posted: 10 October 2018 doi:10.20944/preprints201810.0196.v1

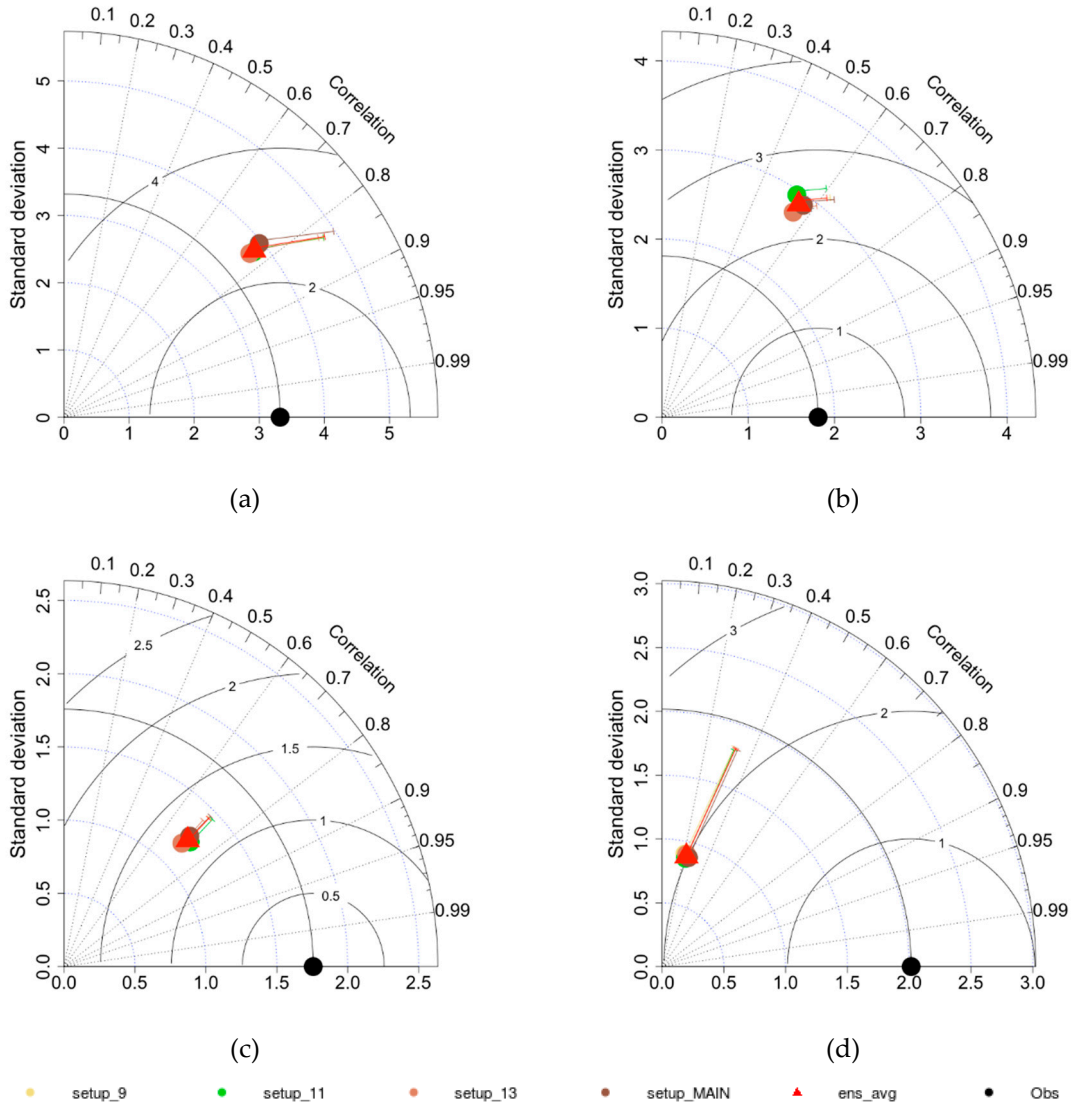

Figure 10. As in Figure 8 except for wind speed at 10m.

4. Discussion

The present study is a two-fold investigation of a Mediterranean cyclone in the western Mediterranean basin. In line with other studies of similar scope, a sensitivity analysis of different physical parameterization schemes for 6 different physics types is carried out [57,58]. In total 15 different model configurations were tested and the results were evaluated against observational data on 3 different parameters: cyclone trajectory, cloud top temperature (CTT) and precipitation rate. The trajectory comparison illustrated a very small to subtle spread among the individual simulations and a rather precise reproduction of the low-pressure center location throughout the lifespan of the cyclone. All sensitivity test simulations were able to reproduce the observed track with a less than 1° difference, concerning mostly a northern offset after the crossing of Sardinia. The results were in line with [5] in which the track analysis displayed good consistency with the observed data in most of the investigated cases. The trajectories and CTT evaluation suggest that the model results are mostly improved when changing the SW/LW radiation, cumulus convection and LSM scheme when compared with the control run. This is partly in agreement to [57] according to which the spread of pressure minima among simulations with different convection and different PBL schemes is smaller than that among simulations with different microphysics.

Validation of the sensitivity test simulations against cloud top BT data obtained by 10.8 μm satellite cloud-top BT revealed values below -50°C (not shown) corresponding to deep convection

 doi:10.20944/preprints201810.0196.v1

over the low-pressure center of the cyclone. The validation against cloud-top temperature observations suggests that WRF performed better when used with different LSM, cumulus and radiation schemes than the defaults (setup_MAIN). On the contrary, changing the default schemes for cloud microphysics, PBL and surface layer led to results less similar to the observations. This is in agreement to [58] which found that Thomson scheme for cloud microphysics, which is the default, performs best. Also, the findings of [27] are confirmed in that the updated version of MYNN (MYNN 2.5) PBL scheme outperforms MYJ scheme in terms of cyclone trajectory, as well as in cyclone depth.

Precipitation analysis sheds light to the deep convection and maximum of precipitation tendency 6-8 hours before the mature phase of the cyclone as described in [57,59–61] revealing the convection weakening and the shallowing of barometric low after the presence of the "eye" on 18/11/2013 at 2200UTC. The consistency with other studies [62,63] thickens the explanation behind the intensification of precipitation on 18/11/2013 at 1500UTC causing the floods that devastated large part of Sardinia.

The second part of the study assesses the forecasting capability of WRF carrying out an ensemble of simulations. The best performing model setups, as determined by the sensitivity tests, were selected for the simulations. In order to achieve maximum variability only one model setup was selected for each kind of model physics parameterization change. The cyclone trajectories of the ensemble forecasting validation as well as the surface validation in Zadar airport, described in section 3.3.2, showed a positive time lag between the model and the satellite trajectory, yet with satisfactory to good precision, when compared to the observed path. Evaluating the cyclone surface pressure minima locations along the tracks, the time lag begun to develop at 36 hours ahead within the 72 hours forecast at the time the cyclone center had crossed the south-east of Sardinia. Along these lines, [57] suggest that the cyclone transition is influenced by a cold front caused by the orography of the area of interest. Similarly, in the present study, the location of the shift and lag of the trajectory indicates the interaction with the occluded front east of Sardinia and also the relatively extreme terrain of the south-east part of the island.

The present study is preliminary work to explore the sensitivity of the numerical simulation of cyclone Cleopatra, using WRF model. The effect of the selection of parameterization schemes combinations, more options of cumulus as well as radiation and PBL schemes have to be examined along with statistical analysis, because they seem to influence significantly model's performance. More sensitivity studies will assist in the identification of the likely best setups exhibiting the most skill for monitoring and forecasting of these complex systems. At the same time, it is important to examine their features and indicators with respect to thermodynamics. Another issue concerns the technique of ensemble forecasting which could also be examined with other proposed methodologies (perturbations) or ensemble means derived from other types of sensitivity tests. Simultaneously, more experiments are carrying out, simulating similar case studies of Mediterranean cyclones in order to study the phenomenon and the performance of the model as the ultimate goal of the project.

5. Conclusions

In the present study, the capability of WRF model in representing the case of the Mediterranean cyclone "Cleopatra" was explored. This cyclone produced some extreme rainfall in Sardinia on 18th November 2013, leading to flash floods with at least 18 casualties as well as rainfall and floods in Calabria, southern Italy. In order to assess the performance of the model a series of 15 sensitivity simulations were performed. The default configuration setup (named "MAIN") was used as base for the other 25 simulations which differed from MAIN in one parameterization scheme of 6 kinds of physical parameterizations.

It was found, consistently with other studies, that by choosing a different than the default scheme for the parameterization of surface layer, PBL or microphysics led to higher errors. in the statistical analysis proposing that MYNN, MYNN 2.5 and Thomson schemes respectively perform the best among the other schemes. The chosen members were setups MAIN, 9,11 and 13 and were derived based on some small discrepancies on their statistical metrics against the remaining performing simulations. CTT validation along with trajectories comparison showed that simulations

using RRTMG, G3D and RUC for radiation, convection and LSM schemes respectively, decreased the model error.

The failure in representing the transition by shifting the forecast cyclone track northwards in the south-east of Sardinia sheds light in the importance of the topography in such an event and how the extreme terrain of this part of the area influences the trajectory forecast.

Overall the forecasting performance of the different model members shows good agreement with observed station data regarding mean sea level pressure, while for wind speed no satisfactory results have been observed for Zadar station, with the lowest correlation coefficient values. Regarding temperature's results, we noticed a more disperse behavior not only between the different setups but also among the different stations.

Finally, WRF forecast develops a positive time lag which commences before the appearance of the northwards deviation of the cyclone track which implies the connection between the shift and the time lag and suggests further investigation similar to [59].

Author Contributions: Conceptualization, M.P.M., K.C.D., I.D.P., N.P., P.T.N.; Methodology, M.P.M., N.P.; Data Curation, M.P.M., I.D.P.; Validation, I.D.P., N.P.; Writing-Original Draft Preparation, M.P.M., K.C.D., I.D.P., N.P., P.T.N.; Supervision, P.T.N.; Project Administration, P.T.N.

Funding: This research is co-financed by Greece and the European Union (European Social Fund- ESF) through the Operational Program «Human Resources Development, Education and Lifelong Learning 2014-2020» in the context of the project "Modelling the Vertical Structure of Tropical-like Mediterranean Cyclones using WRF Ensemble Forecasting and the impact of Climate Change (MEDICANE)" (MIS 5007046).

Acknowledgments: The authors would like to thank the Servizio Meteorologico Aeuronautica Militare of Italy, the Croatian Meteorological and Hydrological Service (DHMZ) and EUMETSAT for the data that were used in order to complete this study. Additionally, the contribution of the European Centre for Medium-Range Weather Forecasts (ECMWF) is acknowledged for the data set provided to initialize the WRF-ARW simulations. Finally, this work has been supported by computational time granted by the GreekResearch and Technology Network (GRNET) in the National HPC facility—ARIS—under projectPR005029-MEDICANE.

Conflicts of Interest: The authors declare no conflict of interest. "The funders had no role in the design of the study; in the collection, analyses, or interpretation of data; in the writing of the manuscript, and in the decision to publish the results.

References

1. Ulbrich, U.; Leckebusch, G. C.; Pinto, J. G. Extra-tropical cyclones in the present and future climate: a review. *Theor. Appl. Climatol.* **2009**, *96*, 117–131, doi:10.1007/s00704-008-0083-8.
2. Flaounas, E.; Raveh-Rubin, S.; Wernli, H.; Drobinski, P.; Bastin, S. The dynamical structure of intense Mediterranean cyclones. *Clim. Dyn.* **2015**, doi:10.1007/s00382-014-2330-2.
3. Cavicchia, L.; Von Storch, H.; Gualdi, S. Mediterranean tropical-like cyclones in present and future climate. *J. Clim.* **2014**, *27*, 7493–7501, doi:10.1175/JCLI-D-14-00339.1.
4. Nastos, P. T.; Karavana Papadimou, K.; Matsangouras, I. T. Mediterranean tropical-like cyclones: Impacts and composite daily means and anomalies of synoptic patterns. *Atmos. Res.* 2017.
5. Miglietta, M. M.; Laviola, S.; Malvaldi, A.; Conte, D.; Levizzani, V.; Price, C. Analysis of tropical-like cyclones over the Mediterranean Sea through a combined modeling and satellite approach. *Geophys. Res. Lett.* **2013**, *40*, 2400–2405, doi:10.1002/grl.50432.
6. Tous, M.; Romero, R. Medicanes: cataloguing criteria and exploration of meteorological environments. *Tethys* **2011**, *8*, 53–61, doi:10.3369/tethys.2011.8.06.
7. Fita, L.; Romero, R.; Luque, A.; Emanuel, K.; Ramis, C. Analysis of the environments of seven Mediterranean tropical-like storms using an axisymmetric, nonhydrostatic, cloud resolving model. *Nat. Hazards Earth Syst. Sci.* **2007**, *7*, 41–56, doi:10.5194/nhess-7-41-2007.
8. Emanuel, K. Genesis and maintenance of "Mediterranean hurricanes." *Adv. Geosci.* **2005**, *2*, 217–220,

476 doi:10.5194/adgeo-2-217-2005.
477 9. Pytharoulis, I.; Craig, G. C.; Ballard, S. P. The hurricane-like Mediterranean cyclone of January 1995.
478 *Meteorol. Appl.* **2000**, *7*, 261–279, doi:10.1016/S1464-1909(99)00056-8.
479 10. Mazza, E.; Ulbrich, U.; Klein, R. The Tropical Transition of the October 1996 Medicane in the Western
480 Mediterranean Sea: A Warm Seclusion Event. *Mon. Weather Rev.* **2017**, *145*, 2575–2595, doi:10.1175/MWR-
481 D-16-0474.1.
482 11. Carrió, D. S.; Homar, V.; Jansa, A.; Romero, R.; Picornell, M. A. Tropicalization process of the 7 November
483 2014 Mediterranean cyclone: Numerical sensitivity study. *Atmos. Res.* **2017**, *197*, 300–312,
484 doi:10.1016/j.atmosres.2017.07.018.
485 12. Cioni, G.; Malguzzi, P.; Buzzi, A. Thermal structure and dynamical precursor of a Mediterranean tropical-
486 like cyclone. *Q. J. R. Meteorol. Soc.* **2016**, *142*, 1757–1766, doi:10.1002/qj.2773.
487 13. Chaboureau, J. P.; Pantillon, F.; Lambert, D.; Richard, E.; Claud, C. Tropical transition of a Mediterranean
488 storm by jet crossing. *Q. J. R. Meteorol. Soc.* **2012**, *138*, 596–611, doi:10.1002/qj.960.
489 14. Hart, R. E. A Cyclone Phase Space Derived from Thermal Wind and Thermal Asymmetry. *Mon. Weather*
490 *Rev.* **2003**, *131*, 585–616, doi:10.1175/1520-0493(2003)131<0585:ACPSDF>2.0.CO;2.
491 15. Homar, V.; Romero, R.; Stensrud, D. J.; Ramis, C.; Alonso, S. Numerical diagnosis of a small, quasi-tropical
492 cyclone over the western Mediterranean: Dynamical vs. boundary factors. *Q. J. R. Meteorol. Soc.* **2003**, *129*,
493 1469–1490, doi:10.1256/qj.01.91.
494 16. Miglietta, M. M.; Cerrai, D.; Laviola, S.; Cattani, E.; Levizzani, V. Potential vorticity patterns in
495 Mediterranean "hurricanes." *Geophys. Res. Lett.* **2017**, *44*, 2537–2545, doi:10.1002/2017GL072670.
496 17. Cavicchia, L.; von Storch, H. The simulation of medicanes in a high-resolution regional climate model. *Clim.*
497 *Dyn.* **2012**, *39*, 2273–2290, doi:10.1007/s00382-011-1220-0.
498 18. Willoughby, H. E.; Rappaport, E. N.; Marks, F. D. Hurricane forecasting: The state of the art. *Nat. Hazards*
499 *Rev.* **2007**, *8*, 45–49, doi:10.1061/(ASCE)1527-6988(2007)8:3(45).
500 19. Pantillon, F. P.; Chaboureau, J.-P.; Mascart, P. J.; Lac, C. Predictability of a Mediterranean Tropical-Like
501 Storm Downstream of the Extratropical Transition of Hurricane Helene (2006). *Mon. Weather Rev.* **2013**, *141*,
502 1943–1962, doi:10.1175/MWR-D-12-00164.1.
503 20. Hart, R. E. A Cyclone Phase Space Derived from Thermal Wind and Thermal Asymmetry. *Mon. Weather*
504 *Rev.* **2003**, *131*, 585–616, doi:10.1175/1520-0493(2003)131<0585:ACPSDF>2.0.CO;2.
505 21. Pytharoulis, I. Analysis of a Mediterranean tropical-like cyclone and its sensitivity to the sea surface
506 temperatures. *Atmos. Res.* **2018**, *208*, 167–179, doi:10.1016/j.atmosres.2017.08.009.
507 22. Romero, R.; Emanuel, K. Climate change and hurricane-like extratropical cyclones: Projections for North
508 Atlantic polar lows and medicanes based on CMIP5 models. *J. Clim.* **2017**, *30*, 279–299, doi:10.1175/JCLI-D-
509 16-0255.1.
510 23. Pytharoulis, I.; Craig, G. C.; Ballard, S. P. The hurricane-like Mediterranean cyclone of January 1995.
511 *Meteorol. Appl.* **2000**, *7*, 261–279, doi:10.1017/S1350482700001511.
512 24. Pytharoulis, I. Analysis of a Mediterranean tropical-like cyclone and its sensitivity to the sea surface
513 temperatures. *Atmos. Res.* 2017, *208*, 167–179.
514 25. Walsh, K.; Giorgi, F.; Coppola, E. Mediterranean warm-core cyclones in a warmer world. *Clim. Dyn.* **2014**,
515 *42*, 1053–1066, doi:10.1007/s00382-013-1723-y.
516 26. Akhtar, N.; Brauch, J.; Dobler, A.; Béranger, K.; Ahrens, B. Medicanes in an ocean-atmosphere coupled
517 regional climate model. *Nat. Hazards Earth Syst. Sci.* **2014**, *14*, 2189–2201, doi:10.5194/nhess-14-2189-2014.
518 27. Ricchi, A.; Miglietta, M. M.; Barbariol, F.; Benetazzo, A.; Bergamasco, A.; Bonaldo, D.; Cassardo, C.; Falcieri,

F. M.; Modugno, G.; Russo, A.; Sclavo, M.; Carniel, S. Sensitivity of a Mediterranean tropical-like Cyclone to different model configurations and coupling strategies. *Atmosphere (Basel).* **2017**, *8*, doi:10.3390/atmos8050092.

28. Davolio, S.; Miglietta, M. M.; Moscatello, A.; Pacifico, F.; Buzzi, A.; Rotunno, R. Numerical forecast and analysis of a tropical-like cyclone in the Ionian Sea. *Nat. Hazards Earth Syst. Sci.* **2009**, *9*, 551–562, doi:10.5194/nhess-9-551-2009.
29. Skamarock, W.; Klemp, J.; Dudhi, J.; Gill, D.; Barker, D.; Duda, M.; Huang, X.-Y.; Wang, W.; Powers, J. A Description of the Advanced Research WRF Version 3. *Tech. Rep.* **2008**, 113, doi:10.5065/D6DZ069T.
30. Hong, S.-Y.; Noh, Y.; Dudhia, J. A New Vertical Diffusion Package with an Explicit Treatment of Entrainment Processes. *Mon. Weather Rev.* **2006**, *134*, 2318–2341, doi:10.1175/MWR3199.1.
31. Mellor, G. L.; Yamada, T. Development of a turbulence closure model for geophysical fluid problems. *Rev. Geophys.* 1982, *20*, 851–875.
32. Pleim, J. E. A combined local and nonlocal closure model for the atmospheric boundary layer. Part I: Model description and testing. *J. Appl. Meteorol. Climatol.* **2007**, *46*, 1383–1395, doi:10.1175/JAM2539.1.
33. NAKANISHI, M.; NIINO, H. Development of an Improved Turbulence Closure Model for the Atmospheric Boundary Layer. *J. Meteorol. Soc. Japan* **2009**, *87*, 895–912, doi:10.2151/jmsj.87.895.
34. Jiménez, P. A.; Dudhia, J.; González-Rouco, J. F.; Navarro, J.; Montávez, J. P.; García-Bustamante, E. A Revised Scheme for the WRF Surface Layer Formulation. *Mon. Weather Rev.* **2012**, *140*, 898–918, doi:10.1175/MWR-D-11-00056.1.
35. Monin, A. S.; Obukhov, A. M. Basic laws of turbulent mixing in the surface layer of the atmosphere. *Contrib. Geophys. Inst. Acad. Sci. USSR* **1954**, *24*, 163–187.
36. Hong, S.; Lim, J. The WRF single-moment 6-class microphysics scheme (WSM6). *J. Korean Meteorol. Soc.* 2006, *42*, 129–151.
37. Thompson, G.; Field, P. R.; Rasmussen, R. M.; Hall, W. D. Explicit Forecasts of Winter Precipitation Using an Improved Bulk Microphysics Scheme. Part II: Implementation of a New Snow Parameterization. *Mon. Weather Rev.* **2008**, *136*, 5095–5115, doi:10.1175/2008MWR2387.1.
38. Chen, F.; Mitchell, K.; Schaake, J.; Xue, Y.; Pan, H.-L.; Koren, V.; Qing Yun, D.; Ek, M.; Betts, A. Modeling of land surface evaporation by four schemes and comparison with FIFI -observations.pdf. *Water Resour. Res.* 1996, *101*, 7251–7268.
39. Chen, F.; Dudhia, J. Coupling an Advanced Land Surface–Hydrology Model with the Penn State–NCAR MM5 Modeling System. Part II: Preliminary Model Validation. *Mon. Weather Rev.* **2001**, *129*, 587–604, doi:10.1175/1520-0493(2001)129<0587:CAALSH>2.0.CO;2.
40. Zhang, Y.; Dulière, V.; Mote, P. W.; Salathé, E. P. Evaluation of WRF and HadRM mesoscale climate simulations over the U.S. Pacific Northwest. *J. Clim.* **2009**, *22*, 5511–5526, doi:10.1175/2009JCLI2875.1.
41. Niu, G. Y.; Yang, Z. L.; Mitchell, K. E.; Chen, F.; Ek, M. B.; Barlage, M.; Kumar, A.; Manning, K.; Niyogi, D.; Rosero, E.; Tewari, M.; Xia, Y. The community Noah land surface model with multiparameterization options (Noah-MP): 1. Model description and evaluation with local-scale measurements. *J. Geophys. Res. Atmos.* **2011**, *116*, doi:10.1029/2010JD015139.
42. Grell, G. A. Prognostic Evaluation of Assumptions Used by Cumulus Parameterizations. *Mon. Weather Rev.* **1993**, *121*, 764–787, doi:10.1175/1520-0493(1993)121<0764:PEOAUB>2.0.CO;2.
43. Kain, J. S. The Kain–Fritsch Convective Parameterization: An Update. *J. Appl. Meteorol.* **2004**, *43*, 170–181, doi:10.1175/1520-0450(2004)043<0170:TKCPAU>2.0.CO;2.
44. Chou, M.-D.; Suarez, M. J. An efficient thermal infrared radiation parameterization for use in general

562 circulation models. *Nasa Tech. Memo* **1994**, *104606*, 85.

563 45. Mlawer, E. J.; Taubman, S. J.; Brown, P. D.; Iacono, M. J.; Clough, S. A. Radiative transfer for
564 inhomogeneous atmospheres: RRTM, a validated correlated-k model for the longwave. *J. Geophys. Res.*
565 *Atmos.* **1997**, *102*, 16663–16682, doi:10.1029/97JD00237.

566 46. Iacono, M. J.; Delamere, J. S.; Mlawer, E. J.; Shephard, M. W.; Clough, S. A.; Collins, W. D. Radiative forcing
567 by long-lived greenhouse gases: Calculations with the AER radiative transfer models. *J. Geophys. Res.*
568 *Atmos.* **2008**, *113*, doi:10.1029/2008JD009944.

569 47. Dudhia, J. Numerical Study of Convection Observed during the Winter Monsoon Experiment Using a
570 Mesoscale Two-Dimensional Model. *J. Atmos. Sci.* **1989**, *46*, 3077–3107, doi:10.1175/1520-
571 0469(1989)046<3077:NSOCOD>2.0.CO;2.

572 48. Fels, S. B.; Schwarzkopf, M. D. The Simplified Exchange Approximation: A New Method for Radiative
573 Transfer Calculations. *J. Atmos. Sci.* **1975**, *32*, 1475–1488, doi:10.1175/1520-
574 0469(1975)032<1475:TSEAAN>2.0.CO;2.

575 49. Collins, W. D.; Rasch, P. J.; Boville, B. A.; Hack, J. J.; Mccaa, J. R.; Williamson, D. L.; Kiehl, J. T.; Briegleb, B.;
576 Bitz, C.; Lin, S.-J.; Zhang, M.; Dai, Y. *Description of the NCAR Community Atmosphere Model (CAM 3.0)*; 2004;

577 50. European Centre for Medium-Range Weather Forecasts ERA5 Reanalysis 2017.

578 51. National Centers for Environmental Prediction NOAA, U.S. Department of Commerce, N. W. S. NCEP
579 GFS 0.25 Degree Global Forecast Auxiliary Grids Historical Archive 2015.

580 52. EUMETSAT European Organisation for the Exploitation of Meteorological Satellites -
581 http://www.eumetsat.int/website/home/index.html.

582 53. Ertürk, A. Msgview : an Operational and Training Tool To Process , Analyze and Visualization of Msg
583 Seviri. **2010**.

584 54. Niedda, M.; Amponsah, W.; Marchi, L.; Zoccatelli, D.; Marra, F.; Crema, S. IL CICLONE CLEOPATRA DEL
585 18 NOVEMBRE 2013 IN SARDEGNA : ANALISI E MODELLAZIONE DELL ' EVENTO DI PIENA The
586 cyclone Cleopatra of November 18 , 2013 in Sardinia , event management , measurement and modelling.
587 *Quad. di Idronomia Mont.* **2013**, 1–13.

588 55. Caloiero, T.; Petrucci, O. the Impact of Damaging Hydrogeological Events on Urbanised Sectors : the Case
589 of 19 Th November 2013 in Catanzaro (Italy). **2014**, 1–8.

590 56. Cavicchia, L.; von Storch, H.; Gualdi, S. A long-term climatology of medicanes. *Clim. Dyn.* **2014**, *43*, 1183–
591 1195, doi:10.1007/s00382-013-1893-7.

592 57. Miglietta, M. M.; Mastrangelo, D.; Conte, D. Influence of physics parameterization schemes on the
593 simulation of a tropical-like cyclone in the Mediterranean Sea. *Atmos. Res.* **2015**, *153*, 360–375,
594 doi:10.1016/J.ATMOSRES.2014.09.008.

595 58. Pytharoulis, I.; Matsangouras, I. T.; Tegoulias, I.; Kotsopoulos, S.; Karacostas, T. S.; Nastos, P. T. Numerical
596 Study of the Medicane of November 2014. In; Springer, Cham, 2017; pp. 115–121.

597 59. Moscatello, A.; Miglietta, M. M.; Rotunno, R. Numerical Analysis of a Mediterranean " Hurricane
598 " over Southeastern Italy. *Mon. Weather Rev.* **2008**, *136*, 4373–4397, doi:10.1175/2008MWR2512.1.

599 60. Conte, D.; Miglietta, M. M.; Levizzani, V. Analysis of instability indices during the development of a
600 Mediterranean tropical-like cyclone using MSG-SEVIRI products and the LAPS model. *Atmos. Res.* **2011**,
601 *101*, 264–279, doi:10.1016/j.atmosres.2011.02.016.

602 61. Laviola, S.; Moscatello, A.; Miglietta, M. M.; Cattani, E.; Levizzani, V. Satellite and Numerical Model
603 Investigation of Two Heavy Rain Events over the Central Mediterranean. *J. Hydrometeorol.* **2011**, *12*, 634–
604 649, doi:10.1175/2011JHM1257.1.

605 62. Davolio, S.; Miglietta, M. M.; Moscatello, A.; Pacifico, F.; Buzzi, A.; Rotunno, R. *Natural Hazards and Earth*
606 *System Sciences Numerical forecast and analysis of a tropical-like cyclone in the Ionian Sea*; 2009; Vol. 9;.
607 63. Claud, C.; Alhammoud, B.; Funatsu, B. M.; Chaboureau, J. P. Mediterranean hurricanes: Large-scale
608 environment and convective and precipitating areas from satellite microwave observations. *Nat. Hazards*
609 *Earth Syst. Sci.* **2010**, *10*, 2199–2213, doi:10.5194/nhess-10-2199-2010.